ISSN(Online) : 2319-8753
ISSN (Print) : 2347-6710

International Journal of Innovative Research in Science, Engineering and Technology

(An ISO 3297: 2007 Certified Organization)

Vol. 4, Issue 7, July 2015

Monitoring and Controlling Locker System Using Skull Identification

T.Indumathi , Dr.M.Pushparani

PhD Scholar, Department of Computer Science, Mother Teresa Women's University, Kodaikannal, India

Professor & Head, Department of Computer Science, Mother Teresa Women's University, Kodaikannal, India

ABSTRACT : Banks provide locker system for their customers for safekeeping. In the current locker system, there is no separate banker to take care and attend to people wishing to access lockers. Every time a customer wishes to access his locker, he must wait until a banker becomes free so that he can authenticate access to the locker. This results in waste of time for both the banker as well as the customer, as the customer has to wait until the banker becomes free and the banker has to stop his work and attend to the customer. The bank security systems are getting more awareness and importance. The Bank Security System is a system for validating, monitoring and controlling the security at bank locker rooms. Today, there are many banks using authorize access control approach to prevent the locker room from unauthorized access. In this paper highly reliable, multi level and most efficient locker room security system has been designed. The system includes a biometric system, i.e. Skull Recognition, which are responsible for the security of the main door of the locker room and the system also includes a RFID system to provide access of the locker room area to only authorize people. To monitor the unauthorized people in the locker room area a passive infrared sensor is fixed. In case of any unauthorized motion the picture from the camera will be mailed to security officials and the alarms will be on to inform the local security. The system proposed in this paper is a better security system in terms of number of level of security. The project aims to change the system and automate the locker system using RFID tags for customer identification. Every customer is given a unique RFID card with a unique number so that the customer can be identified and access can be granted to the customer's locker. The RFID card is activated in the Micro controller, created the pin number,the image capture the Camera verification of customer by matching the distance of the top, left, right, bottom of the human Face. The image can be applying active appearance model algorithm, it is converted the mesh.

The proposed a method is AAM using the canonical correlation analysis (CCA), which has modeled the relation between differences of the image and the model parameter for improving the convergence speed of algorithm. The skull of the CT scan be store in database, CT image converted in 3D images for mesh for applying marching cub algorithm.human face is captured by the pseudo 3D image capture at the camera. The feature points are calculated and encrypted and sent to the server via a secure channel. The encryption is based on bio keys. If the value matches with the encoded value in the database, it allows locker open.

KEYWORDS: RFID System, Biometric System, Passive Infrared Sensor , skull verification, encryption, decryption.

I. INTRODUCTION

Increasing incidence of crimes against banks has necessitated a serious re-look at the security arrangements and guidelines followed by the banks. Increase in anti social activities is a cause of concern as the banks are considered soft targets by criminal. The prevailing crime scenario demands compatible, efficient and reliable security and safety measures. In this security system the specific persons can only enter. by using this embedded system we can give access to the authorized people through the finger print modules and keypads. The system is programmable we can change the data of the authorized people in the data base of the embedded system. We can access the data on the embedded system on to computer. This is the main disadvantage.

The first system will be placed at the front door of the locker room area and another will be placed at the gate of the locker room. Most doors are generally manually controlled by the security person employed by the bank with the use of

ISSN(Online) : 2319-8753
ISSN (Print) : 2347-6710

International Journal of Innovative Research in Science, Engineering and Technology

(An ISO 3297: 2007 Certified Organization)

Vol. 4, Issue 7, July 2015

handle locks operated by a key. In this system each user will be provided with a unique RFID card. The front door will open only when a authorize person wants to enter with an authorize card. In the locker room area a passive infrared sensor will be mounted with a camera. In case if a person gets enter at the locker room area without any authorize card then a passive infrared sensor is actively waiting for it, which will send a signal to a microcontroller and the microcontroller will take two actions, first it will switch on the alarms which will inform the local security and second it will take a snapshot of the locker room area and mail it to the authorize person using a personal computer. The second system which is placed at the locker room entrance consist a biometric system. To open the gate of the locker room the person needs to get his/her face Recognition(The skull of the human face is captured by the pseudo 3D image capture at the camera) to be verified and converting to some digital format, The back-end system (database) to compare the values and store the template values. When these processes will complete, only then the locker room will be opened.

The proposed a fast AAM using the canonical correlation analysis (CCA), which has modeled the relation between differences of the image and the model parameter for improving the convergence speed of fitting algorithm. Moreover,have proposed an efficient AAM algorithm based onthe inverse compositional image alignment algorithm. This approach did not demand a linear relationship between the differences of image and the model parameter. However, this model has outperformed the conventional AAM in terms of yielding better fitting accuracy; furthermore the proposed model has also got faster convergence.

In this paper, we propose to identify an unknown skull through using a correlation measure between the 3D skull and 3D face in terms of the morphology, and measure the correlation using canonical correlation analysis (CCA) [13]. We use the 3D skull data as the probe and 3D face geometric data as the gallery, and match the unknown skull with enrolled 3D faces by the correlation measure between the probe and the gallery. Considering that the strength of the correlation between the skull and face in different craniofacial regions is not the same, we propose a region fusion strategy to measure the correlation between the skull and face more reliably and to boost the identification capability. The proposed method reduces the complexity of the skull identification problem. Unlike craniofacial superimposition and craniofacial recon-struction, it is not necessary to have an accurate relationship between the skull and face; the system measures only the correlation between them. The contributions of this paper are as follows: Firstly, a novel and reliable skull identification technique is presented, and to the best of our knowledge, it is the first time that such a technique has been reported. Secondly, this paper proves that there is indeed a close relation between the skull and face in terms of the morphology, and thus, it provides a theory support for related research, i.e. craniofacial superimposition and craniofacial reconstruction.

II. RELATED WORK

Fuqing Duan, Yanchao Yang, Yan Li, Yun Tian, Ke Lu, Zhongke Wu, and Mingquan Zhou , published a paper on "Skull Identification via Correlation Measure Between Skull and Face Shape" where they proposed In this paper, we propose a novel technique for identifying an unknown skull based on the correlation measure between the 3D skull and 3D face in terms of the morphology. Using the 3D skull data as the probe and 3D face geometric data as the gallery, this approach matches the unknown skull with enrolled 3D faces by the correlation measure between the probe and the gallery. Unlike craniofacial superimposition and craniofacial reconstruction, this method does not require an accurate relationship between the skull and face.

Junli Zhao,1,2 Cuiting Liu,1 ZhongkeWu,1 Fuqing Duan,1Kang Wang,1 Taorui Jia,1 and Quansheng Liu3 "Craniofacial Reconstruction Evaluation by Geodesic Network" where they proposed This paper proposes an objective method to evaluate globally and locally the reconstructed craniofacial faces based on the shape index of geodesic network vertices.
The geodesic networks of the craniofacial faces are built by geodesics and isogeodesics. For each geodesic network vertex, we define the weighted average of the shape index value in a neighborhood as the feature of the network vertex.

Yongli Hu1, Fuqing Duan2, Mingquan Zhou2, Yanfeng Sun1* and Baocai Yin1 "Craniofacial reconstruction based on a hierarchical dense deformable model "where they proposed We proposed a hierarchical dense deformable model for

ISSN(Online) : 2319-8753
ISSN (Print) : 2347-6710

International Journal of Innovative Research in Science, Engineering and Technology

(An ISO 3297: 2007 Certified Organization)

Vol. 4, Issue 7, July 2015

automatic craniofacial reconstruction. The feature of proposed model is that the skull and face are represented as dense mesh without landmarks. The advantage of this representation is that the dense meshes contain more meta-data for exploring the intrinsic relation between skull and face. In addition, the presented non-rigid dense meshes registration and the model matching procedure can be implemented automatically, which contributes to the fully automatic craniofacial reconstruction method

Michael Kistler _, Marcel Pfahrer y, Roman Niklaus y, Viktor Tomasy and Philippe Buechler "The Virtual Skeleton Database: An open access repository for biomedical research and collaboration" where they proposed The VSD is a flexible system equipped with an ontology powered search, compelling collection of full body datasets. The system proved its value and concept of being a genericrepository by hosting an Tumor Segmentation Challenge online.The registration, data management and sharing functionality were used without any change to the VSD and the system provides the required background processing.

Hamdan.O.Alanazi, B.B Zaidan, A.A Zaidan, published a paper on "3D skull recognition using 3D matching Technique" where they proposed a technique to recognize a person with the picture of the skull of this person. On that paper they used a 3D detection technique for recognizing the skull. In their research project they choose a 3D square for matching in the first stage. In the second stage they choose a 3D human skull. They choose three different points in the skull and then tried to calculate the number of matching pixel. By this process they tried to locate a particular human or a particular person.

Shihab A Hameed, B. B. Zaidan, A.A. Zaidan, A.W Naji and Omar Farooq published a paper named "Novel simulation Framework of three-dimensional Skull bio-metric Measurement", where they showed how a 3D image of a person can be recognized using simulated system.In their research project they choose a 3D skull for matching. For the simulation they use Canfield Imaging Systems. These systems providean environment where the researchers can simulate a 3D skull for visualize, analyze and measure (VAM) different properties of that particular skull. In their research they took a 3D skull and match it with another 3D skull. If both the skulls match then those skulls are actually same skull.

Zane Krisjane, Ilga Urtane, Gaida Krumina, Anvita Bieza, Katrina Zepa, Irena RoGovska published a paper named "Condylar and mandibular morphological criteria in the 2D and 3D MSCT imaging for patients with class II division I subdivision malocclusion" where they try to develop an algorithm valid for the quantification of morphological structure and skeletal landmarks of the condyle, processus condylaris and mandible in patient with class II division I subdivision malocclusion. In their research they used 2D MSCT and 3D MSCT (Multi-sliced Computed Tomography) imaging system. By the help of this system they measure different type of distance of mandible.

SHUI Wuyang,ZHOU Mingquan, DENG Qingqiong, WU Zhongke, DUAN Fuqing published a paper on" 3D Craniofacial Reconstruction using Reference Skull-Face Database".In this paper, aiming at the craniofacial reconstruction for a Chinese unidentified skull, an approach to estimate the outlook of the skull is presented and a method of evaluating the result is introduced. The skull-face database of Chinese is established and classified based on age, gender and area. For the choice reference template, a method to determine the correspondence points is presented and then the no rigid registration is achieved to outlook estimation. For the subclass template, the PCA statistic model is built and the accurate result is estimated. Finally, organ and face integration technology is used to estimate more exact outlook of the unidentified skull.

Sourav Ganguly, Subhayan Roy Moulick published a paper on "Proposed Mathematical Model for Face Recognization of a Human from Lower Jaw or Mandible" These papers presenting some approaches for recognize a human face from skull. It is introduced here to recognize a person by the help of the lower jaw or mandible of that person. The proposed mathematical model will try to find out the solution for the problem.

III. SYSTEM HARDWARE COMPONENTS

This section will illustrate us brief idea about the main components which are going to be used in this security system and their functionalities.

ISSN(Online) : 2319-8753
ISSN (Print) : 2347-6710

International Journal of Innovative Research in Science, Engineering and Technology

(An ISO 3297: 2007 Certified Organization)

Vol. 4, Issue 7, July 2015

A. Microcontroller Atmega16

Atmega16 is a low power CMOS 8 bit microcontroller. It is based on RISC architecture. The RISC architecture consists of 131 powerful instructions set in which most of the instruction are of one clock cycle. It has 32x8 general purpose registers and it can give throughput of 6 MIPS at 16 MHz. It has on chip comparator, 8 channel of 10 bit analog to digital convertors, separate on chip oscillator, two 8 bit and one 16 bit timer/counter, programmable watch dog timer, four PWM channels and 16kb self programmable flash memory.

In this security system 3 different Atmega16 microcontrollers have been used as shown in figure 1. Microcontroller 1 and 2 are interfaced with each other. Microcontroller 1 is working like a master and it is responsible to activate the microcontroller 2 and open the front door of locker room area. Microcontroller 3 is responsible to open the main door of the locker

B. RFID System

RFID stands for Radio Frequency Identification System which is an intelligent bar code technology. The advantage of RFID system over bar code technology is that it does not require line of sight. The RFID system supports a large number of unique IDs with additional data storage. Data in a RFID system can be changed and updated which provides it flexibility. The RFID system basically consist two things, one is tag and other one is tag reader. Each tag has a unique 12 to 16 digit identification number. The tag reader is responsible for powering up and communicating with a tag. When the tag is placed on the tag reader, the reader captures the energy and reads the identification number and transfers it.

The RFID system is further connected to the microcontroller via the serial port as shown in figure 1. The tag IDs are already stored in the microcontroller where the matching is performed.

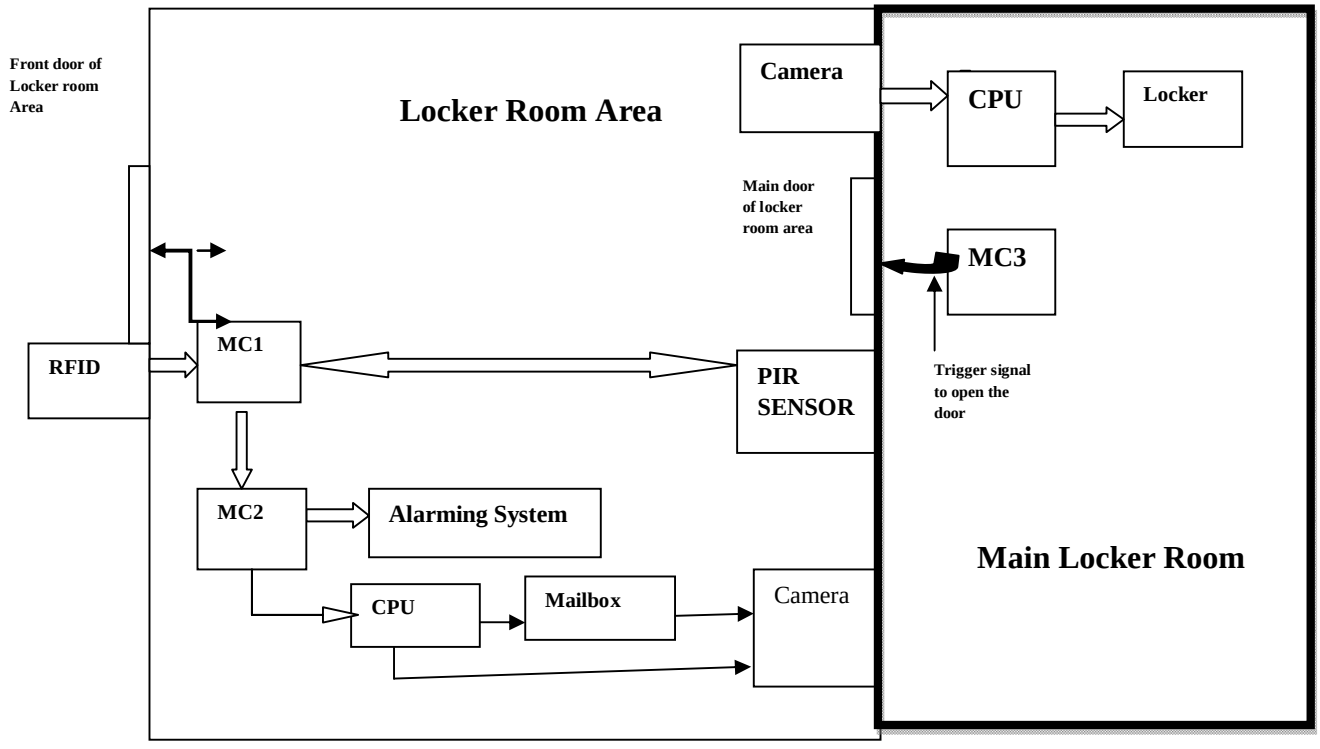

Figure 1. The Basic Architecture of Bank Security System

ISSN(Online) : 2319-8753
ISSN (Print) : 2347-6710

International Journal of Innovative Research in Science, Engineering and Technology

(An ISO 3297: 2007 Certified Organization)

Vol. 4, Issue 7, July 2015

C. Biometric System

The image of the skull is taken by the pseudo-3D Image capture at the camera and is encrypted using the bio key and translate the encrypted value to the database. If the value in the template of the database matched with the current encrypted value, the locker can be opened.

C.1 Material

The original CT slice images were processed by the Sobel operator model after filtering out the noise to extract the skull and face borders. The 3D skull and skin surfaces are reconstructed by a marching cubes algorithm [25], and they are represented as triangle meshes that include approximately 1 50,000 and 2 20,000 vertices, respectively. All of the heads are substantially complete. In detail, each skull contains all of the bones from calvarias to jaw and has a full mouth of teeth, and no face has a missing part. In addition, the subject's properties for each head, such as the age, gender, and body mass index (BMI), are stored. All of the information is self-reported by the participants. More of the details on the procedure for the data processing can be found in.

To eliminate the inconsistency in the position, pose and scale caused by data acquirement, all of the samples are transformed into a uniform coordinate system. The uniform coordinate system is determined by four skull landmarks, the left porion, right porion, the left (or right) orbitale and the glabella (denote as Lp, Rp, Lo, G). From three points, Lp, Rp, Lo, the Frankfurt plane is determined [22]. The coordinate origin (denoted as O) is the intersection point of the line LpRp and the plane that contains point G and orthogonally intersects the line LpRp. We take the line ORp as the x −axis. The z−axis is the line through the point O, and it has the direction of the normal of the Frankfurt plane. Then, the y−axis is obtained by the cross product of the z− and x −axis. Once the uniform coordinate system is defined, all of the prototypic skins and skulls are transformed into it by a simple rotation and translation transformation. Finally, the scale of all of the samples is standardized by setting the distance between Lp and Rp to a unit, i.e., each vertex (x, y, z) of the skull and skin is scaled by $L^p - R^p$. The skull and face skin of one sample in the uniform coordinate system are shown in Figure.2. The original skull and skin meshes have different connectivity. In statistical learning, a dense point

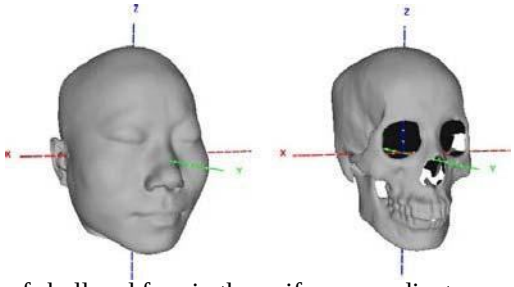

Fig. 2. One pair of skull and face in the uniform coordinates system.

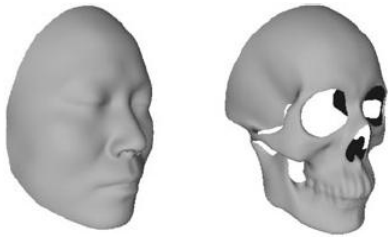

Fig. 3. The reference skull and face skin for data registration.

Correspondence must be established across the training set. As is known, the representation capability of statistical models depends critically on the quality of the correspondence. An inappropriate correspondence can cause the variation modes of the statistical model to not reflect the actual variation of the objects. Although there are many data registration methods for dense mesh or point cloud objects to establish the point correspondence, it is still a challenging problem to obtain accurate registration for dense skull and face meshes because there are complex non-rigid

ISSN(Online) : 2319-8753
ISSN (Print) : 2347-6710

International Journal of Innovative Research in Science, Engineering and Technology

(An ISO 3297: 2007 Certified Organization)

Vol. 4, Issue 7, July 2015

deformations among different craniofacial subjects. Here, we adopt the dense registration method described in . It includes two steps. The first step is a non-rigid registration procedure using a fixed reference. The second step is to improve the registration by a linear combination model based on the first-step registered samples. This method reduces the model bias caused by a fixed reference at the cost of higher computational complexity. Fortunately, we do not need a real-time registration. Similar to the literature , we select one skull-and-face pair as a reference and cut away their back parts, considering that face recognition mainly depends on the front part of the head. As shown in Figure 3, the reference skull and face have 41,059 and 40,969 vertices, respectively. After the data registration, all of the skulls and face skins have the same mesh connectivity as the reference one.

IV. METHODS

In skull identification, nearly all of the methods depend on accurate extraction and representation of the relationship between the skull and face. However, it is very difficult to extract this complex relationship. Because this work aims to identify an skull by looking for its corresponding face skin from a 3D face gallery, we measure only the correlation between a skull and a face skin, and do not need an accurate relationship.

A. Statistical Shape Model

Principal Component Analysis (PCA). In our experiments we implemented Principal Component Analysis (PCA) procedure as described by Turk and Pentland (1991). Given an s-dimensional vector representation of each face in a training set of M images, PCA tends to find a t-dimensional subspace whose basis vectors correspond to the maximum variance direction in the original image space. This new subspace is normally lower dimensional (t << s).New basis vectors define a subspace of face images called face space. All images of known faces are projected onto the face space to find sets of weights that describe the contribution of each vector. To identify an unknown image, that image is projected onto the face space as well to obtain its set of weights. By comparing a set of weights for the unknown face to sets of weights of known faces, the face can be identified. If the image elements are considered as random variables, the PCA basis vectors are defined as eigenvectors of the scatter matrix S_T defined as:

$$S_T = \sum_{i=1}^{M} (xi - \mu).(xi - \mu)T \quad (1)$$

where μ is the mean of all images in the training set (the mean face, Fig. 4) and xi is the ith image with its columns concatenated in a vector.

The projection matrix W_{PCA} is composed of t eigenvectors corresponding to t largest eigenvalues, thus creating a t-dimensional face space. Since these eigenvectors (PCA basis vectors) look like some ghostly faces they were conveniently named eigenfaces .

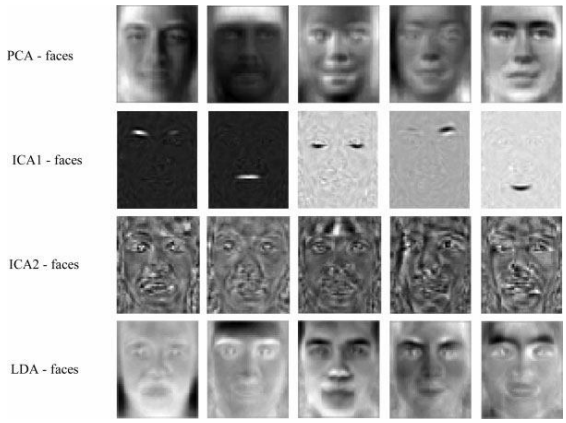

Fig.4 PCA and LDA Faces

ISSN(Online) : 2319-8753
ISSN (Print) : 2347-6710

International Journal of Innovative Research in Science, Engineering and Technology

(An ISO 3297: 2007 Certified Organization)

Vol. 4, Issue 7, July 2015

B Active Appearance Model:

Feature Extraction Using AAM Modeling. Given a set of training images, $Ii\ (x, y)$, $x = 0, 1, \ldots, n-1$, $y = 0, 1, \ldots, m-1$,
and $i = 0, 1, \ldots, N-1$, where $Ii\ (x, y)$ is of size $N \times M$. In the training images, the active portions have been manually labelled for extracting the parameters of the shape and appearance models.

In a 2D image landmark points can be represented as a 2n shape vector, X, where $X = (x1, \ldots, xn, y1, \ldots, yn)T$. The set of shape vectors have been normalized to a common reference frame; hence X can be represented by x and by applying PCA:

$S = S + Fs$, (4)

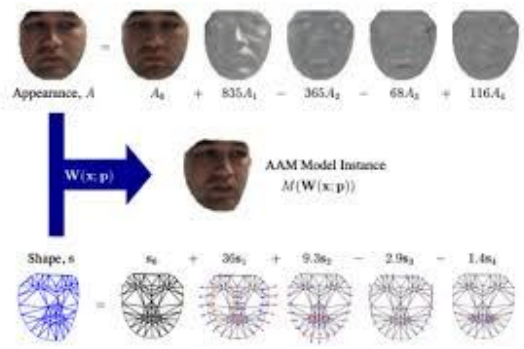

Fig.5 AAM modal

where S represents the synthesized shape in the normalized frame, S illustrates the mean shape in the normalized frame, Fs depicts the matrix of eigenvectors, extracted from the training shape, and ns is a set of shape parameters. In Fig5. after acquiring a shape model, every single training image has been distorted, where its control factors could match the mean shape. Next, the information is tested from the shape-normalized image, which is encompassed by the mean shape for forming a texture vector, G. A texture model might be constructed by applying PCA to the normalized texture vectors,
$G = G + Fg$, (5)
where G is the synthesized texture in the normalized frame, G is the mean texture in the normalized frame, Fg is the matrix which contains eigenvectors as columns, and ng is a set of texture parameters. The example of shape and texture can be synthesized by ns and ng . Since there are correlations between shape and texture variations, a weight matrix, should be
established for each shape parameter. Ws is a diagonal scaling matrix. Then a concatenated vector can be generated:
$l = ({}_{ng}{}^{Ws}{}^{)=}\ (_{Fg\ (G-G)}{}^{Ws\ Fs\ T\ (S-S)})$. (6)

An appearance model will be set up by using a further PCA,
$l = Qa$, Q=($_{Qg}{}^{Qs}$), (7)
where Q is the matrix which contains the eigenvectors as columns and a is a set of appearance parameter. Now a shape and texture model can be expressed by the appearance parameter, a,
$S = S + Fs\ Ws\ Qs\ a$, $G = G + Fg\ Qg\ a$. (8)

C.HCCA in the Shape Parameter Spaces

As described above, each training skull or face skin can be projected into its shape parameter space. That is, each skull has p feature variables, while each face skin has q feature variables. Let $\mathbf{X}_{N \times p}$ and $\mathbf{Y}_{N \times q}$ denote the training skull and face data matrices, respectively, and let N denote the size of the training samples. The aim of HCCA is to find two sets

ISSN(Online) : 2319-8753
ISSN (Print) : 2347-6710

International Journal of Innovative Research in Science, Engineering and Technology

(An ISO 3297: 2007 Certified Organization)

Vol. 4, Issue 7, July 2015

of basis vectors, $\mathbf{w}_x \in R^p$ and $\mathbf{w}_y \in R^q$, that maximize the correlation coefficient between the components $\mathbf{t}_1 = \mathbf{X}\mathbf{w}_x$ and $\mathbf{u}_1 = \mathbf{Y}\mathbf{w}_y$, i.e.,

$$\rho = \max_{w_x, w_y} \frac{\mathrm{cov}(t_1, u_1)}{\sqrt{\mathrm{Var}(t_1) \times \mathrm{Var}(u_1)}} = \max_{w_x, w_y} \frac{w_x^T C_{xy} w_y}{\sqrt{w_x^T C_{xx} w_x \times w_y^T C_{yy} w_y}}$$

where the covariance matrices $\mathbf{C}_{xy} = \mathbf{X}^T\mathbf{Y}$, $\mathbf{C}_{xx} = \mathbf{X}^T\mathbf{X}$ and $\mathbf{C}_{yy} = \mathbf{Y}^T\mathbf{Y}$.

Let $\mathbf{W} = \mathbf{w}_x^T, \mathbf{w}_y^T{}^T$ and $\mathbf{C}_{yx} = \mathbf{Y}^T\mathbf{X}$, then Equation (4) can be solved by computing a generalized eigen-value decomposition problem, as follows:

$$\mathbf{AW} = \lambda \mathbf{BW} \qquad (9)$$

where

$$\mathbf{A} = \begin{pmatrix} \mathbf{0} & C_{xy} \\ C_{yx} & \mathbf{0} \end{pmatrix}, \quad \mathbf{B} = \begin{pmatrix} C_{xx} & \mathbf{0} \\ \mathbf{0} & C_{yy} \end{pmatrix}. \qquad (10)$$

More details on the derivation and solution of CCCA can be found in [13].

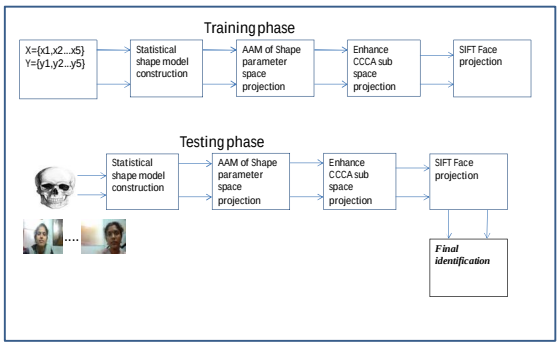

Fig. 6 Hcca based skull identification

Thus, we obtain two subspaces that consist of the basis vectors $\mathbf{w}_x \in R^p$ and $\mathbf{w}_y \in R^q$, respectively, for the skull and face skin. Assume that $\mathbf{W}_x$ denotes the subspace projection matrix whose columns are the basis vectors $\mathbf{w}_x$, and $\mathbf{W}_y$ is the matrix that corresponds to the basis vectors $\mathbf{w}_y$. For a skull-and-face pair, let $\mathbf{x}$ denote the shape parameter vector of the skull, and let $\mathbf{y}$ denote the shape parameter vector of the face. Then, the feature vectors of the skull and face in the CCCA subspaces are

$$\begin{aligned} xc &= WxT\ x \\ yc &= WTy\ y. \end{aligned} \qquad (11)$$

ISSN(Online) : 2319-8753
ISSN (Print) : 2347-6710

International Journal of Innovative Research in Science, Engineering and Technology

(An ISO 3297: 2007 Certified Organization)

Vol. 4, Issue 7, July 2015

We define the matching score between the skull and face as follows:

$$r(xc,yc)=xc,yc \quad xc,yc \qquad (12)$$

E Architecture for Encrypt and Comparison

Encryption process is used to convert the PIN number and feature points to unreadable form (cipher text). Initially the RFID Card open the locker room area require bank and gets the PIN number to access it. The image of the customer's skull is taken and feature points are calculated. The feature point value is encrypted using the bio key and stored in the database along with the PIN number. It does not require the separate database to store the feature point values. Comparisons of skull feature values are made the locker opened.

F. *Architecture for Decryption*

Decryption is the reverse of encryption. The values are decrypted and then compared. Decryption process is carried out using the same bio key. It compares the values and allow for door opened when the values are matched. Else it decline.

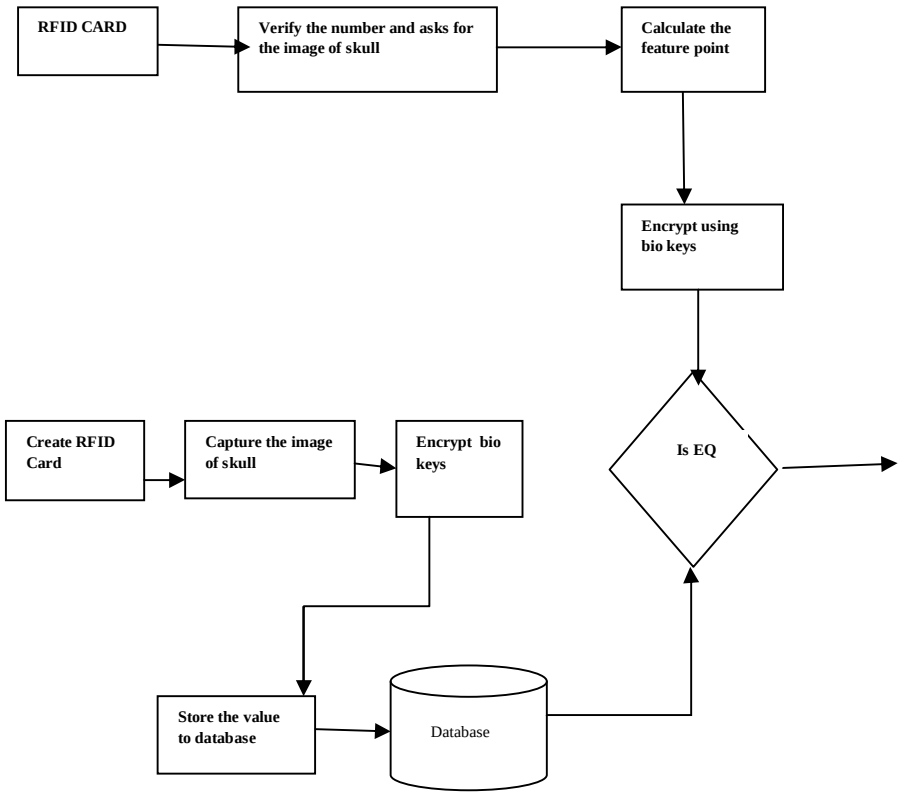

Figure 7. The Basic Architecture for Encrypt and Comparison

G. Passive Infrared Sensor

The passive infrared sensor is basically a motion sensor which is used to detect that an object is moving in or out of the sensor range. It consists a crystalline material at the center of a rectangle called pyroelectric sensor, which is able to detect levels of infrared detection. The PIR sensors detect infrared radiation from an object that generates heat and hence infrared radiation within its range. The PIR sensors are cut into two halves such that it does not detect radiation

ISSN(Online) : 2319-8753
ISSN (Print) : 2347-6710

International Journal of Innovative Research in Science, Engineering and Technology

(An ISO 3297: 2007 Certified Organization)

Vol. 4, Issue 7, July 2015

from itself, but when the target enters in the field the change in condition occurs. These changes in term of infrared radiation converted in the form of voltage by the use of the supporting circuitry of resistors and capacitors. The voltage value is read by the ADC of the microcontroller. If the input voltage crosses the threshold value then the object is detected. When an object is detected, a high output signal is driven to the MCU of the microcontroller. The range of the PIR sensor is 6 meters which is enough to detect any motion in the locker room area. The advantage of using PIR sensor is that it is small, inexpensive, low power, rugged, with a high range, easy to interface and easy to use.

V. SYSTEM OPERATION

The flow chart of operation of security system has been given in figure 8. As already written the complete system has been divided in two parts which has been shown as a partial line in the figure7. The system 1 will be responsible for the security of the entrance to the locker room area i.e. the front door of the locker room area.

When a person wants to enter to the locker room area he or she needs to place the authorized RFID tag on the card reader. When the correct match is found using microcontroller1 then it will deactivate the already activated PIR sensor so as to avoid misunderstanding. The microcontroller1 will now open the front door of locker room area for a specified time. If any unauthorized motion is occurred then the PIR will detect this motion and it will send a signal back to the microcontroller1. Microcontroller1 will activate the slave microcontroller2. Once microcontroller2 will be activated then it will activate the alarming system; which will inform the local security about the unauthorized motion and send a signal to the CPU. The CPU consists of MATLAB codes which will force the camera placed at the corner of the locker room area to take a snapshot revert that back to the CPU. Now the further MATLAB codes will send that picture to the mailbox of the authorized person.

The security evaluation of the person wants to enter not only ends here. The system 2 will be responsible for the security to the entrance of the locker room i.e. main door of the locker room. A person needs to get his/her iris scanned using the scanner. If the match found correctly using the CPU then the person will go under another scanning process which is the fingerprint scanning. If the match found correctly again using the CPU then a signal will be sent to the microcontroller3; which will now open the main door of the locker room for a specified time. In this way the security system will provide security to the locker room at different layers.

ISSN(Online) : 2319-8753
ISSN (Print) : 2347-6710

International Journal of Innovative Research in Science, Engineering and Technology

(An ISO 3297: 2007 Certified Organization)

Vol. 4, Issue 7, July 2015

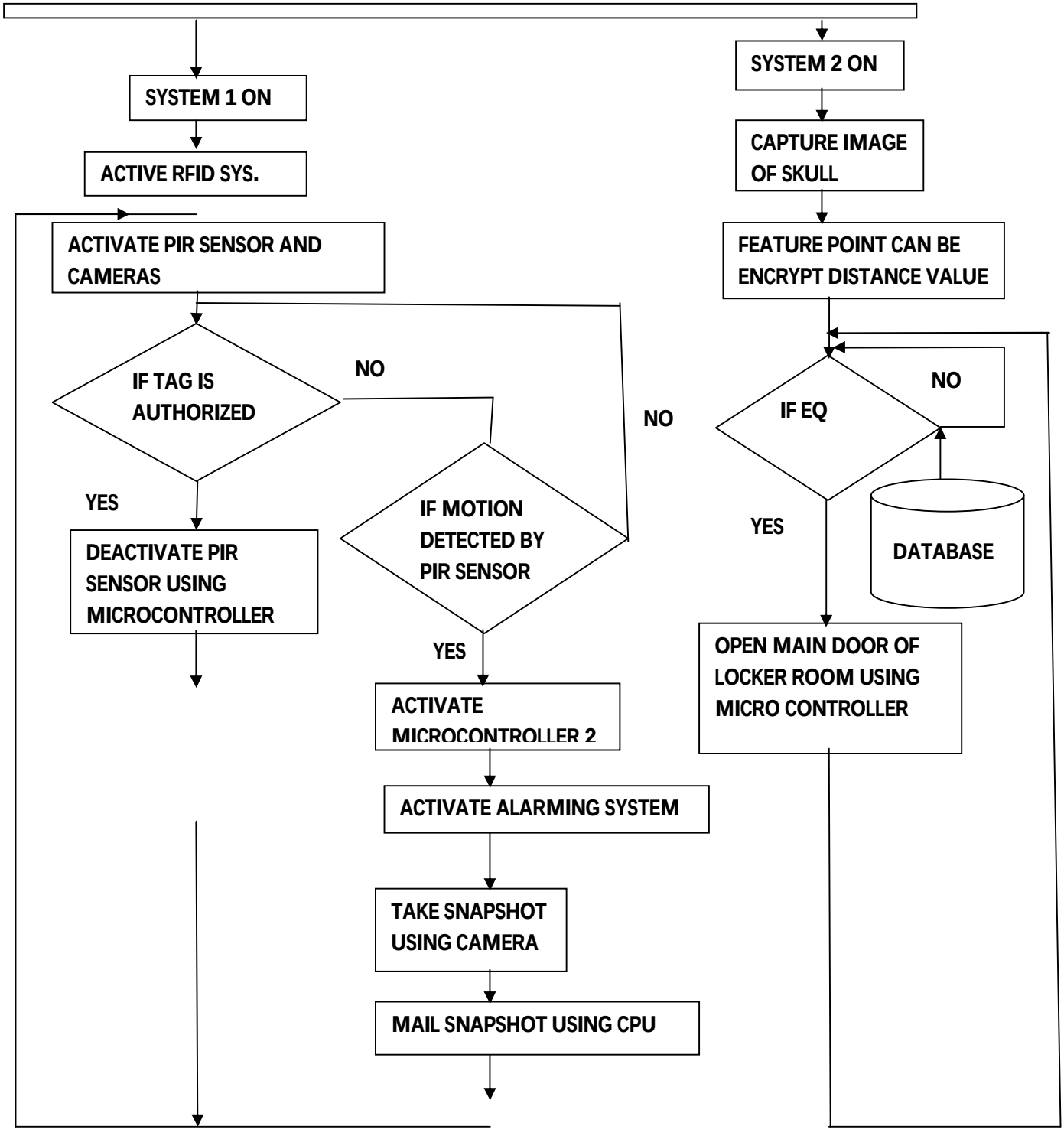

Figure 8. The Flow Chart of System Operation

ISSN(Online) : 2319-8753
ISSN (Print) : 2347-6710

International Journal of Innovative Research in Science, Engineering and Technology

(An ISO 3297: 2007 Certified Organization)

Vol. 4, Issue 7, July 2015

VI.RESULT AND DISCUSSION

The used dataset is the 3D skull-and-face skin pairs of the 250 subjects described in Section II. Five-fold cross-validation was used to evaluate the proposed method. We randomly chose 7 non-overlapping data groups from the dataset, and each group included the 3D skull-and-face skin pairs of 30 subjects. For each fold, 30skulls in one group were used as probes to test the proposed method, and the remaining 120 pairs of skull-and-face skins constitute the training set. In other words, we have 275 test skulls in all five folds. For each test skull, all of the 220 face skins constitute the gallery. The correct identification rate reported in the experiments is the average of the five folds. In this paper, we define that a test skull is identified at rank *n*, if the matching score of the correct match is of rank *n*. The identification rate at rank *n* is defined as the ratio of the cumulative count of the numbers of test skulls identified at rank *n* or less to the total number of test skulls. The correct identification rate is defined as the identification rate at rank.

I.Evaluation of skull identification using LDA and PCA:

Both Linear Discriminant Analysis (LDA) and Principal Component Analysis (PCA) are linear transformation techniques that are commonly used for dimensionality reduction. PCA can be described as an "unsupervised" algorithm, since it "ignores" class labels and its goal is to find the directions (the so-called principal components) that maximize the variance in a dataset. In contrast to PCA, LDA is "supervised" and computes the directions ("linear discriminants") that will represent the axes that maximize the separation between multiple classes.In Fig.9compare the shape parameter.in the following table1.

Table 1 shape parameter LDA AND PCA

Region	Profile	Forehead	Eye	nose	Mouth
Skull	74	67	30	33	65
Face	50	45	30	41	55

Although it might sound intuitive that LDA is superior to PCA for a multi-class classification task where the class labels are known, this might not always be the case.

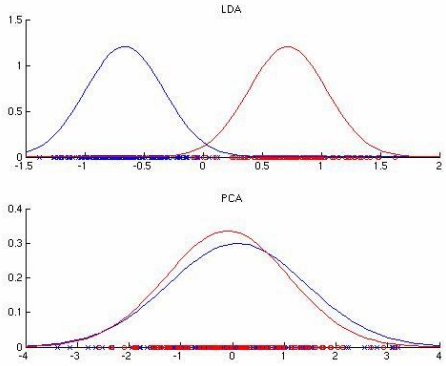

Fig. 9 Compare of PCA and LDA

Section IV is discussed for shape parameter in skull and face. The PCA shape of face recognize the database, to identify unknown image, that image is projected onto the face space as well to obtain its set of weights. By comparing a set of weights for the unknown face to sets of weights of known faces, the face can be identified. If LDA shape and near the PCA and maximizing the component axes for face space.

II.Evaluation of skull identification using Enhance canonical correlation coefficient analysis.

For each fold, we built a enhance correlation analysis model in which all of the 176 eigen-vectors are used to construct the statistical shape models. A total of 150 test skulls were correctly identified at rank 1. The correct identification rate

ISSN(Online) : 2319-8753
ISSN (Print) : 2347-6710

International Journal of Innovative Research in Science, Engineering and Technology

(An ISO 3297: 2007 Certified Organization)

Vol. 4, Issue 7, July 2015

attained 81.5%. It verifies that there indeed exists some relationship between the skull and face, and it also shows that the proposed skull identification method is effective.

To describe the confidence evaluation of the identification result presented in Section IV, four test groups in four folds are used to estimate the probability distributions of the positive matching (i.e., the matching between a skull with its corre-sponding face) and the negative matching (i.e., the matching between a skull with the faces of other persons), and the identification results of the 40 test skulls in the remaining one fold are used for the confidence evaluation. In this part, the former four test groups are referred to as the probability training set, while the latter 40 test skulls are referred to as the evaluation set. We perform statistical analysis for the 25600 ($4 \times 40 \times 160$) matching scores that were derived from the probability training set. The mean and standard deviation are (0.3205, 0.0811) for the positive matching and (0.0009, 0.0806) for the negative matching. Figure 6a and 6b show the histograms of the matching scores for the positive and negative matching, respectively. From Figure 6, we can see that both the positive and negative matching score approximately follow a Gaussian distribution. Thus, the two class conditional probability density functions can be set as Gaussian distributions, with the mean and standard deviation computed for the positive and negative matching, respectively. Figure 9c shows the two stan-dard Gaussian distributions. We can see that the scores of the positive and negative matching are separable. The conditional

probability $P(w_1| E)$ in Equation (14) can be set as the average correct identification rate of the four folds that the probability training set belongs to, i.e., 80.6%. The prior probability $P(E)$ can be set to 1 because all of the face data of the test skulls exists in the face gallery in this experiment. According to the Bayes decision rule, we evaluate the identification results of the evaluation set, i.e., the 40 test skulls in the remaining one fold. Five of the 6 false identification results and all of the 34 correct results are classified as positive. If we set $P(E)$ as 0.5, i.e., we have no prior information about whether the face data of the test skull exists in the face gallery, then one correct identification result is classified as negative and 3 false results are classified as positive.

By performing analysis of there are two cases for the false identification skulls. One case is that both the correct matching score and the mismatched score are low, and this case can be classified as negative matching.

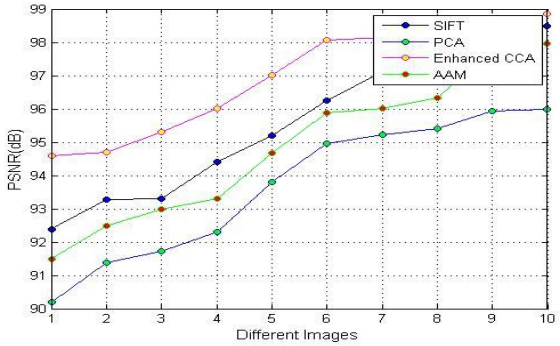

Fig. 10. CCA compare performance (a)skull and image gallery of cca (b)Comparsion of pca,lda,cca

ISSN(Online) : 2319-8753
ISSN (Print) : 2347-6710

International Journal of Innovative Research in Science, Engineering and Technology

(An ISO 3297: 2007 Certified Organization)

Vol. 4, Issue 7, July 2015

Table 2 organ

Region	profile	Forehead	nose	Mouth
Identification rate	76%	81	35	20

Table3 correlation coefficient analysis

region	Profile	Forehead	Eye	nose	mouth
Skull	85	77	65	75	85
Face	75	75	80	81	85

The other case is that the global morpho-logical similarity between the mismatched face and the true face is high, and it can be misclassified as positive matching. Figure 10 shows two samples of the second case. We can see that the mismatched faces are visually similar to the true faces. Figure10 also shows the comparison colored from blue to red according to the geometric distance between the two faces. The average distances of these two samples are 2.7 mm and 2.56 mm, respectively. From the colored comparisons, we can see that the distance between the mismatched faces and the true faces is very small in most of the regions. The global morphological similarity between two faces leads to similar shape model parameters, which contribute to the false matching due to a holistic model. For this reason, we propose the region-based method.

VII. CONCLUSIONS

This project has the potential to greatly reduce the manpower required during the access of bank lockers by the customers and also greatly saves time for both the banker and the customer. Bank locker room security is an emerging need throughout the world. Time is considerably saved by this RFID based automated bank locker system as there is no need for any authentication by the bank employee. In this paper we have designed two systems that allow unlocking a protected door. The paper has successfully presented a functional, low complexity microcontroller based low cost multi layer security system. The real life model of the prototype can be designed with minimum designing cost and with relatively low operational cost for bank locker rooms where high degree of security is required. In near future more number of security levels can be added for monitoring as well as control. The security can be used in other highly restricted areas also like private offices, laboratories etc.

REFERENCES

1. W. E. Lorensen and H. E. Cline, “Marching cubes: A high resolution 3D surface construction algorithm,” *ACM SIGGRAPH Comput. Graph.*, vol. 21, no. 4, pp. 163–169, 1987.
2. Q. Deng, M. Zhou, W. Shui, Z. Wu, Y. Ji, and R. Bai, “A novel skull registration based on global and local deformations for craniofacial reconstruction,” *Forensic Sci. Int.*, vol. 208, nos. 1–3, pp. 95–102, 2011.
3. W. Yang, D. Yi, Z. Lei, J. Sang, and S. Z. Li, “2D–3D face matching using CCA,” in *Proc. 8th IEEE Int. Conf. Autom. Face Gesture Recognit. (FG)*, Sep. 2008, pp. 1–6.
4. B. Abraham and G. Merola, “Dimensionality reduction approach to multivariate prediction,” *Comput. Statist. Data Anal.*, vol. 48, no. 1, 5–16, 2005.
5. W. Zheng, X. Zhou, C. Zou, and L. Zhao, “Facial expression recognition using kernel canonical correlation analysis (KCCA),” *IEEE Trans. Neural Netw.*, vol. 17, no. 1, pp. 233–238, Jan. 2006.
6. P. J. Besl and N. D. McKay, “A method for registration of 3-D shapes,” *IEEE Trans. Pattern Anal. Mach. Intell.*, vol. 14, no. 2, pp. 239–256, Feb. 1992.
7. P. Tu, R. Book, X. Liu, N. Krahnstoever, C. Adrian, and P. Williams, “Automatic face recognition from skeletal remains,” in *Proc. IEEE Conf. Comput. Vis. Pattern Recognit. (CVPR)*, Jun. 2007, pp. 1–7.
8. J. Huang, M. Zhou, F. Duan, Q. Deng, Z. Wu, and Y. Tian, “The weighted landmark-based algorithm for skull identification,” in *Proc. 14th Int. Conf. Comput. Anal. Images Patterns (CAIP)*, LNCS 6855. 2011, pp. 42–48.
9. Y. Hu, F. Duan, M. Zhou, Y. Sun, and B. Yin, “Craniofacial reconstruc-tion based on a hierarchical dense deformable model,” *EURASIP J. Adv. Signal Process.*, vol. 2012, p. 217, Oct. 2012.
10. G. M. Gordon and M. Steyn, “An investigation into the accuracy and reliability of skull-photo superimposition in a South African sample,” *Forensic Sci. Int.*, vol. 216, nos. 1–3, pp. 198.e1–198.e6, 2012.
11. Fuqing Duan, Yanchao Yang, Yan Li, Yun Tian, Ke Lu, Zhongke Wu, and Mingquan Zhou” Skull Identification via Correlation Measure

ISSN(Online) : 2319-8753
ISSN (Print) : 2347-6710

International Journal of Innovative Research in Science, Engineering and Technology

(An ISO 3297: 2007 Certified Organization)

Vol. 4, Issue 7, July 2015

Between Skull and Face Shape" IEEE transactions on information forensics 8and security, vol. 9, no. 8, august 2014

12. W. Yang, D. Yi, Z. Lei, J. Sang, and S. Z. Li, "2D–3D face matching using CCA," in *Proc. 8th IEEE Int. Conf. Autom. Face Gesture Recognit. (FG)*, Sep. 2008, pp. 1–6.
13. D. R. Hardoon, S. Szedmak, and J. Shawe-Taylor "Canonical correlation analysis: An overview with application to learning methods," *Neural Comput.*, vol. 16, no. 12, pp. 2639–2664, 2004.
14. L. Ballerini, O. Cordón, J. Santamaria, S. Damas, I. Aleman, and M. Botella, "Craniofacial superimposition in forensic identification using genetic algorithms," in *Proc. 3rd Int. Symp. Inf. Assurance Security*, 2007, pp. 429–434.
15. O. Ibáñez, L. Ballerini, O. Cordón, S. Damas, and J. Santamaría, "An experimental study on the applicability of evolutionary algorithms to craniofacial superimposition in forensic identifcation," *Inf. Sci.*, vol. 179, no. 23, pp. 3998–4028, 2009.
16. T. W. Fenton, A. N. Heard, and N. J. Sauer, "Skull-photo superimposi-tion and border deaths: Identification through exclusion and the failure to exclude," *J. Forensic Sci.*, vol. 53, no. 1, pp. 34–40, 2008.
17. J. Santamaria, O. Cordón, S. Damas, and O. Ibaez, "Tackling the coplanarity problem in 3D camera calibration by means of fuzzy land-marks: A performance study in forensic craniofacial superimposition," in *Proc. IEEE 12th Int. Conf. Comput. Vis. Workshop (ICCV)*, Oct. 2009, pp. 1686–1693.
18. O. Ibáñez, O. Cordón, S. Damas, and J. Santamaría, "Modeling the skull–face overlay uncertainty using fuzzy sets," *IEEE Trans. Fuzzy Syst.*, vol. 19, no. 5, pp. 946–959, Oct. 2011.
19. D. Vandermeulen, P. Claes, D. Loeckx, S. De Greef, G. Willems, and P. Suetens, "Computerized craniofacial reconstruction using CT-derived implicit surface representations," *Forensic Sci. Int.*, vol. 159, pp. S164–S174, May 2006.
20. S. Michael and M. Chen, "The 3D reconstruction of facial features using volume distortion," in *Proc. 14th Eurograph. U.K. Conf.*, 1996, pp. 297–305.
21. P. Claes, D. Vandermeulen, S. De Greef, G. Willems, J. G. Clement, and P. Suetens, "Bayesian estimation of optimal craniofacial reconstruc-tions," *Forensic Sci. Int.*, vol. 201, nos. 1–3, pp. 146–152, 2010.
22. Y. Hu *et al.*, "A hierarchical dense deformable model for 3D face reconstruction from skull," *Multimedia Tools Appl.*, vol. 64, no. 2, 345–364, 2013.